Joint Modelling of Structural and Functional Brain Networks

Kasper Winther Andersen[1,2], Tue Herlau[1], Morten Mørup[1], Mikkel N. Schmidt[1], Kristoffer H. Madsen[2], Mark Lyksborg[1,2], Tim B. Dyrby[2], Hartwig R. Siebner[2], and Lars Kai Hansen[1]

[1] DTU Informatics, Technical University of Denmark
[2] Danish Research Centre for Magnetic Resonance, Copenhagen University Hospital Hvidovre

Abstract. Functional and structural magnetic resonance imaging have become the most important noninvasive windows to the human brain. A major challenge in the analysis of brain networks is to establish the similarities and dissimilarities between functional and structural connectivity. We formulate a non-parametric Bayesian network model which allows for joint modelling and integration of multiple networks. We demonstrate the model's ability to detect vertices that share structure across networks jointly in functional MRI (fMRI) and diffusion MRI (dMRI) data. Using two fMRI and dMRI scans per subject, we establish significant structures that are consistently shared across subjects and data splits. This provides an unsupervised approach for modeling of structure-function relations in the brain and provides a general framework for multimodal integration.

1 Introduction

While the dominant paradigm in neuroimaging remains functional localization, there is much current interest in understanding the mechanisms behind brain wide coordination in more complex human behaviors. Network representations and graph theoretical analyses offer new means to understand functional coordination both under normal behaviors and pathology. Current brain imaging technology offers multiple views on these networks and it has been suggested that structural information obtained via diffusion MRI (dMRI) and information from functional MRI (fMRI) can be combined in a synergistic way to produce a more complete picture, see e.g., [4, 7, 18, 10, 8, 12, 16].

Existing work on combining functional connectivity and structural connectivity is based on comparing or correlating results obtained from each method independently [13, 6]. This includes comparisons of descriptive measures of structural and functional networks like the distribution of motifs or other global properties, such as the link distribution, small world properties, or degree of modularity, for a recent review see [16]. However, in order to fully benefit from the individual advantages of each modality thereby improving detection power and explicitly capture shared network structure, models that are able to integrate both types on information in the same framework are needed. This is indeed the aim of recent work on informing functional clustering by measures of structural connectivity as derived from dMRI [3]. This so-called anatomically weighted functional clustering method (awFC) produces more strongly autocorrelated functional networks compared with conventional unweighted functional clustering of time series.

Here, we set up an expressive generative model that can potentially learn the structure-function relation locally. The new model is formulated in a new Bayesian non-parametric multi-graph modeling framework that allows for arbitrary relations between a set of modules also determined by data and most importantly directly models the potential integration between structure and function at the node level. In particular, we propose a non-parametric generative model that divides nodes into two types *i) shared nodes that exhibit the same clustering structure across modalities* and *ii) individual nodes (not shared) that are clustered differently across modalities*. This admits the analysis of shared and individual structures in networks with multiple link types, i.e., graphs defined by functional and structural connectivity respectively (see also Figure 1(a)) and the investigation of the structure-function relationship in brain networks and provides a general framework for multimodal integration.

To validate our approach we train and test on two separate sets of structural and functional MRI graphs obtained for a total of 22 subjects. We compare with a model that assumes there are no clusters shared between the functional and structural connectivity graphs and a model that assumes clusters are fully shared between the functional and structural connectivity graphs. In addition, we investigate if subjects are better modelled by subject specific partitions of the brain regions compared to partitions that are the same across subjects.

2 Methods

Consider a set of graphs $\big\{G_{n,m}\big(V, E_{n,m}\big) : n \in \{1,\dots,N\}, m \in \{1,\dots,M\}\big\}$, each defined on the same set of vertices $V = \{v_1,\dots,v_K\}$. The set of graphs is indexed by (n, m) where the former in the present context refers to whether the graph is derived from functional or diffusion MRI ($N = 2$) and the latter refers to different subjects or repetitions.

2.1 Generative model

We propose the following model for the set of graphs: For each vertex v_i, a Bernoulli variable J_i indicates whether its linking properties are shared across graphs, $J_i = 0$, or are individual for each graph, $J_i = 1$. According to a Chinese restaurant process (CRP), the set of shared vertices $V_{\text{sh.}} = \{v_i : J_i = 0\}$ is divided into a partition Z_0 represented by $\{z_i^{(0)}\}_{i\in V_{\text{sh.}}}$ where $z_i^{(0)}$ is an index of the cluster to which vertex v_i belongs. For each $n \in \{1,\dots,N\}$ the set of individual nodes $V_{\text{in.}} = \{v_i : J_i = 1\}$ is divided into a partition Z_n represented by $\{z_i^{(n)}\}_{i\in V_{\text{in.}}}$. For each graph in the set, a link probability variable $\eta_{\mu,\nu}^{(n,m)}$ determines the probability of observing a link $A_{i,j}^{(n,m)}$ in the graph $G_{n,m}$ between two vertices v_i and v_j belonging to cluster μ and ν respectively. The full generative model is described in Figure 1(b). The tunable parameters of the model are $\psi = \{\kappa, \ell, \alpha, \gamma, \delta\}$ and they were all set to unity in our experiments.

The model posits a stochastic block structure which is identical across subjects / repetitions (m) but only partially shared across network types (n). Since the degree of shared block structure is variable, the model allows us to learn from data to what extent

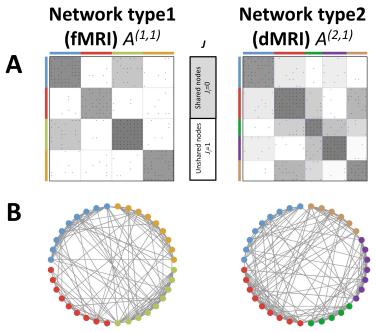

(a)

1) Draw the probability of nodes being shared:

$$\phi \sim \text{Beta}(\kappa, \ell)$$

2) For each node draw a binary variable J_i indicating whether the node is shared or individual:

$$\forall i \; J_i \sim \text{Bernoulli}(\phi)$$

3) For the shared nodes draw cluster assignments:

$$\forall i : J_i = 0 \; \{z_i^{(0)}\} \sim \text{CRP}(\alpha)$$

4) For the individual nodes draw cluster assignments:

$$\forall n, i : J_i = 1 \; \{z_i^{(n)}\} \sim \text{CRP}(\alpha)$$

5) For individual and shared clusters draw link probability:

$$\forall n, m, \mu, \nu : \mu \leq \nu \; \eta_{\mu,\nu}^{(n,m)} \sim \text{Beta}(\gamma, \delta)$$

6) For all subjects and network types draw links:

$$\forall n, m, i, j : i < j \; A_{i,j}^{(n,m)} \sim \text{Bernoulli}(\eta^{(n,m)}_{z_i^{(n \cdot J_i)}, z_j^{(n \cdot J_j)}})$$

(b)

Fig. 1. (a) Schematic model description. Panel A shows the adjacency matrices for two network types. The small black dots indicate edges. Grouping structures are indicated with colors to the left and above the adjacency matrices and group link probabilities are indicated with the gray-scaled background. In this example nodes belonging to the first two modules are shared across network type while the remaining nodes show different grouping in the two networks. Panel B gives a graphical layout of the networks where nodes are shown with filled circles and edges as lines. The color indicate the same grouping structure as in panel A. (b) Proposed generative model.

common block structure is present across different types of networks. We further consider two special cases of this partially-shared block model: A fully-shared $J_i = 1 \; \forall i$ and a fully-unshared $J_i = 0 \; \forall i$ model. In the fully-shared model a single partitioning of the nodes is shared between all graphs; however, the link probabilities remain separate for each graph allowing the model to capture shared group structure despite differences in link densities. The type of model has previously been considered in [14]. In the fully-unshared model each graph is assumed independent, and our model reduces to N independent multi-graph infinite relational models (IRM) [11].

2.2 Data acquisition

We use fMRI and dMRI data obtained from 22 healthy volunteers.

Functional MRI: Resting state functional magnetic resonance imaging (rs-fMRI) data was recorded for 20 min (482 volumes) per subject. The first two volumes were discarded to account for T1 equilibrium effects, the remaining 480 volumes were realigned to the time-series mean and spatially normalized to the MNI template using SPM8. Nuisance effects related to residual movement or physiological effects were removed. In order to enable the characterization of reproducibility and predictive likelihood, the fMRI data was blocked into 6 equally sized blocks each consisting of 80 non-overlapping volumes. For each subject the 6 blocks was randomly split into two independent datasets each containing 3 blocks. For each of the two datasets the mean signal in each of the 116 regions as defined in the AAL database [17] was extracted and a $[116 \times 116]$ correlation matrix was formed for each of the datasets for each subject.

Diffusion MRI: Each subject underwent two diffusion weighted imaging (DWI) sessions. For each session diffusion along 61 directions were recorded with $b = 1200$s/mm^2. Additionally, 10 $b = 0$ images were obtained. To compensate for subject motion and Eddy currents artifacts, the DWI volumes of each subject were aligned with the first DWI volume (b-value=0) using an affine image transformation [5]. The displacements of the affine transformations were combined with the displacement maps of SPM8's Fieldmap approach [9], and displacement maps correcting for the non-linearity of the scanner gradients, resulting in a single resampling for each volume, achieved using cubic interpolation. The rotational parts of the affine transformations are extracted and gradient directions corrected using the Finite Strain approach [1]. FSL's Bedpostx was used to estimate voxelwise diffusion parameters for each subjects' two DWI sessions. Bedpostx uses Markov Chain Monte Carlo sampling to build distributions of the diffusion parameters and allows for detection of crossing fibres. FSL's probtrackx [2] was used for probabilistic tractography. The AAL brain regions were normalized to each subject's native space and used for seeding and target regions. For each voxel a distribution of 5000 pathway samples was generated and the average count of pathways to each region was used to generate the connectivity matrix $\boldsymbol{C}$. In order to generate un-directional graphs we average $\tilde{\boldsymbol{C}} = \frac{1}{2}(\boldsymbol{C} + \boldsymbol{C}^\top)$.

Construction of graphs: The correlation matrix derived from fMRI and the averaged pathway count matrix derived from dMRI were thresholded to form binary adjacency matrices. The threshold was selected such that the resulting graph had a specific link density. We experimented with graph densities between 0.5 % and 50 %.

3 Results and discussion

3.1 Analysis of fMRI and dMRI data

We consider two types of analysis of the data. A modeling where fMRI and dMRI are modelled jointly for each subject individually (i.e. $M = 1$) as well as a population study where all subjects are modelled in the same model ($M = 22$).

The result of the analysis of the individual subjects (i.e., $M = 1$) is given in figure 2 where the mean and standard deviation of the fraction of shared vertices across fMRI and dMRI, area under the receiver operating characteristic curve (AUC), predictive log-likelihood ($\log L^{\text{test}}$), number of clusters, and MI are given. Figure 2 show that the $\log L^{test}$ and AUC scores in the partial-shared model is on par with the best performing of the fully-unshared and fully-shared models. Furthermore, the modeling benefits the most from partially sharing vertices at a graph density of 3% where about 60% of the vertices in both data splits are shared, interestingly this is the suggested density level for analysis proposed by [15]. Finally the number of components for the partial-shared model and the mutual information falls between the fully-unshared and the fully-shared models. The modeling of all subjects jointly (i.e., $M = 22$) gave similar results and are therefore not included.

In figure 2(b) we also compare the AUC score of a model that considers each subject individually ($m = 1$) with a model which models all subjects combined ($m = 22$)(black lines). In general the all-subjects model lie well above the individual-model and thus

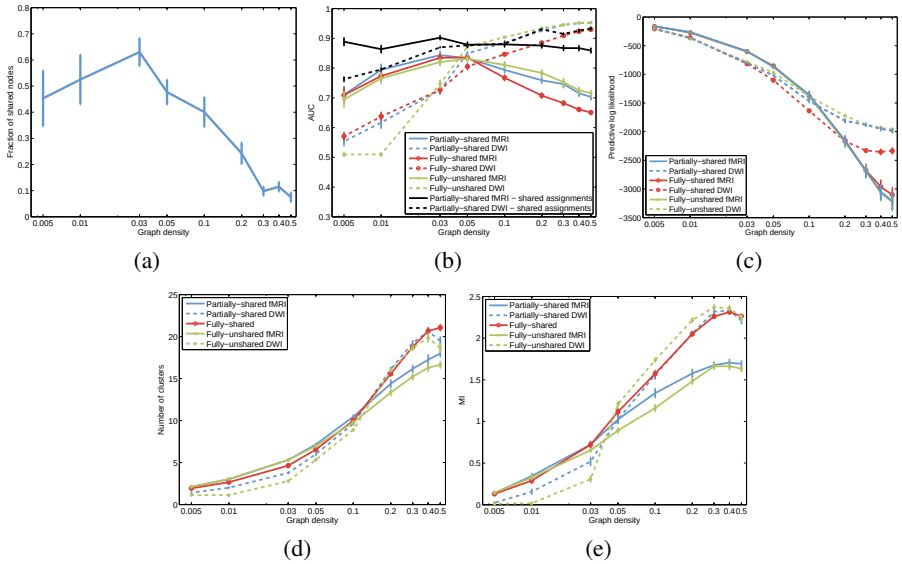

(a) (b) (c)

(d) (e)

Fig. 2. (a) fraction of shared nodes as function of graph density for the partially-shared model; (b) AUC score; (c) predictive log likelihood; (d) number of clusters; (e) mutual information (MI) between sessions.

indicate that models with the same node partition over subjects are better at predicting network structure and thereby also indicates that it is a good assumption that the node-partition can be shared across subjects.

In figure 3 the frequency that each vertex of the brain is shared across fMRI and dMRI on average across all subjects for the individual analysis (i.e., $M = 1$) and population study (i.e., $M = 22$) are given for the two data splits. The same regions are consistently shared across the two data splits as well as across the individual and population studies. Red signifies regions that are significantly shared and blue regions that are significantly unshared across the subjects. The significance level is evaluated relative to a null model where vertices are randomly sampled as shared based on a Bernoulli distribution with success defined by the subject specific fraction of vertices shared for the individual study ($M = 1$) and for the estimated fraction of vertices shared across subjects in the population study (i.e., $M = 22$) respectively. The significance level has been corrected for multiple comparisons using the Dunn-Šidák correction. The regions that are significantly shared primarily constitute cerebellum and frontal lobe whereas regions that are significantly different in fMRI and dMRI are found in the parietal and temporal lobes.

4 Conclusion

Integration of the different modalities of structural and functional connectivity data remains a difficult challenge for computational neuroscience. We have proposed a frame-

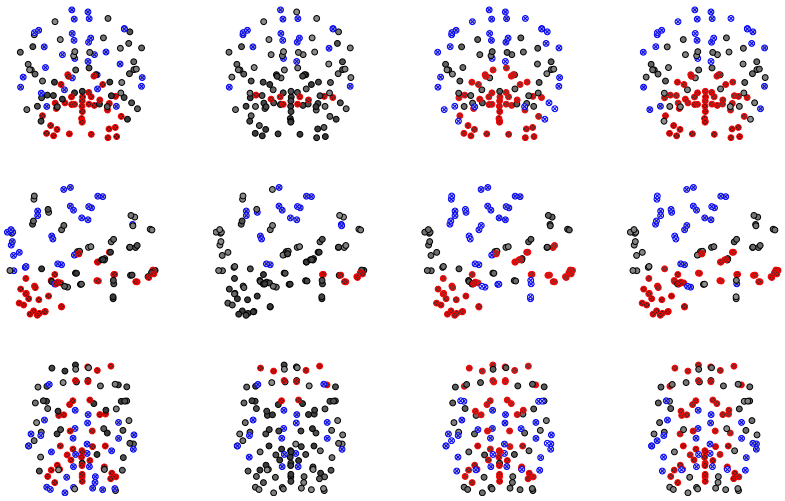

Fig. 3. Frequency of shared vertices across fMRI and dMRI for session1 and session2 computed for individual subjects (i.e. $M = 1$) (two first columns) and session1 and session2 computed for the population study (i.e. $M = 22$) (two last columns). Red signifies regions that are significantly shared and blue regions that are significantly unshared across the subjects.

work which allows for joint modelling of different network types and inference of vertices which share structure.

The model was evaluated on fMRI and dMRI data derived from 22 subjects. Using two scans of each data type per subject we demonstrated the inferred structure and patterns of shared vertices could be recovered in a reliable way both across data splits and within subjects, specifically we demonstrated (i) significant sharing in the cerebellum and frontal cortex as well as significantly differences in parietal and temporal lopes (ii) the model was on par with the best performing fully-shared and fully-unshared models in link-prediction and the number of components and mutual information fell between the fully-unshared and fully shared models. Finally, we observed that the model which shares node partitions across subjects better predicts network structure than models with individual subject node partitions.

Our model provides a principled unsupervised framework for establishing structure-function relationship in brain networks. We believe this is a crucial property for models of the relation between these data modalities and it may advance our understanding on the relationship between the functional and structural organization of the brain in both healthy and clinical populations.

References

1. D. C. Alexander, C. Pierpaoli, P. J. Basser, and J. C. Gee. Spatial transformations of diffusion tensor magnetic resonance images. *Medical Imaging, IEEE Transactions on*.
2. T. E. J. Behrens, M. W. Woolrich, M. Jenkinson, H. Johansen-Berg, R. G. Nunes, S. Clare, P. M. Matthews, J. M. Brady, and S. M. Smith. Characterization and propagation of uncer-

tainty in diffusion-weighted MR imaging. *Magnetic resonance in medicine: Official journal of the Society of Magnetic Resonance in Medicine / Society of Magnetic Resonance in Medicine*, 50(5):1077–88, Nov. 2003.

3. F. D. Bowman, L. Zhang, G. Derado, and S. Chen. Determining Functional Connectivity usying fMRI Data with Diffusion-Based Anatomical Weighting. *NeuroImage*, May 2012.
4. E. Bullmore and O. Sporns. Complex brain networks: graph theoretical analysis of structural and functional systems. *Nature Reviews Neuroscience*, 10(3):186–198, 2009.
5. A. Collignon, F. Maes, D. Delaere, D. Vandermeulen, P. Suetens, and G. Marchal. Automated multi-modality image registration based on information theory. In *Information processing in medical imaging*, volume 3, pages 264–274, 1995.
6. M. Filippi and F. Agosta. Structural and functional network connectivity breakdown in Alzheimers disease studied with magnetic resonance imaging techniques. *Journal of Alzheimer's disease : JAD*, 24(3):455–74, Jan. 2011.
7. M. Guye, G. Bettus, F. Bartolomei, and P. J. Cozzone. Graph theoretical analysis of structural and functional connectivity MRI in normal and pathological brain networks. *Magma (New York, N.Y.)*, Mar. 2010.
8. C. J. Honey, O. Sporns, L. Cammoun, X. Gigandet, J. P. Thiran, R. Meuli, and P. Hagmann. Predicting human resting-state functional connectivity from structural connectivity. *Proceedings of the National Academy of Sciences*, 106(6):2035, 2009.
9. P. Jezzard and R. S. Balaban. Correction for geometric distortion in echo planar images from bo field variations. *Magn Reson Med*, 34(1):65–73, 1995.
10. H. Johansen-Berg, T. E. J. Behrens, M. D. Robson, I. Drobnjak, M. F. S. Rushworth, J. M. Brady, S. M. Smith, D. J. Higham, and P. M. Matthews. Changes in connectivity profiles define functionally distinct regions in human medial frontal cortex. *Proceedings of the National Academy of Sciences of the United States of America*, 101(36):13335, 2004.
11. C. Kemp, J. B. Tenenbaum, T. L. Griffiths, T. Yamada, and N. Ueda. Learning systems of concepts with an infinite relational model. In *Proceedings of the national conference on artificial intelligence*, volume 21, page 381, 2006.
12. T. R. Knösche and M. Tittgemeyer. The role of long-range connectivity for the characterization of the functional–anatomical organization of the cortex. *Frontiers in systems neuroscience*, 5, 2011.
13. M. J. Lowe, E. B. Beall, K. E. Sakaie, K. A. Koenig, L. Stone, R. A. Marrie, and M. D. Phillips. Resting state sensorimotor functional connectivity in multiple sclerosis inversely correlates with transcallosal motor pathway transverse diffusivity. *Hum.Brain Mapp.*, 29(1097-0193 (Electronic) LA - eng PT - Journal Article PT - Research Support, Non-U.S. Gov't SB - IM):818–827, July 2008.
14. K. T. Miller, T. L. Griffiths, and M. I. Jordan. Nonparametric latent feature models for link prediction. *Advances in Neural Information Processing Systems (NIPS)*, pages 1276–1284, 2009.
15. M. Rubinov and O. Sporns. Complex network measures of brain connectivity: uses and interpretations. *NeuroImage*, 52(3):1059–1069, 2010.
16. O. Sporns. The human connectome: a complex network. *Annals of the New York Academy of Sciences*, 1224(1):109–125, 2011.
17. N. Tzourio-Mazoyer, B. Landeau, D. Papathanassiou, F. Crivello, O. Etard, N. Delcroix, B. Mazoyer, and M. Joliot. Automated anatomical labeling of activations in SPM using a macroscopic anatomical parcellation of the MNI MRI single-subject brain. *NeuroImage*, 15(1):273–289, Jan. 2002.
18. Z. Zhang, W. Liao, H. Chen, D. Mantini, J. Ding, Q. Xu, Z. Wang, C. Yuan, G. Chen, Q. Jiao, et al. Altered functional–structural coupling of large-scale brain networks in idiopathic generalized epilepsy. *Brain*, 134(10):2912–2928, 2011.